ISSN 1674-1056
http://cpb.iphy.ac.cn
http://iopscience.iop.org/cpb
中国物理 B
Chinese Physics
中国物理 Chinese Physics B

Concept study of measuring gravitational constant using superconducting gravity gradiometer

Xing Bian(边星), Ho Jung Paik, Martin Vol Moody

Citation: Chin. Phys. B . 2018, 27(8): 080401. **doi:** 10.1088/1674-1056/27/8/080401

Journal homepage: http://cpb.iphy.ac.cn; http://iopscience.iop.org/cpb

What follows is a list of articles you may be interested in

An efficient calibration method for SQUID measurement system using three orthogonal Helmholtz coils

Hua Li(李华), Shu-Lin Zhang(张树林), Chao-Xiang Zhang(张朝祥), Xiang-Yan Kong(孔祥燕), Xiao-Ming Xie(谢晓明)

Chin. Phys. B . 2016, 25(6): 068501. **doi:** 10.1088/1674-1056/25/6/068501

Levitation and lateral forces between a point magnetic dipole and a superconducting sphere

H M Al-Khateeb, M K Alqadi, F Y Alzoubi, B Albiss, M K Hasan (Qaseer), N Y Ayoub

Chin. Phys. B . 2016, 25(5): 058402. **doi:** 10.1088/1674-1056/25/5/058402

Stability of magnetic tip/superconductor levitation systems

M. K. Alqadi

Chin. Phys. B . 2015, 24(11): 118404. **doi:** 10.1088/1674-1056/24/11/118404

Low-T_c direct current superconducting quantum interference device magnetometer-based 36-channel magnetocardiography system in a magnetically shielded room

Qiu Yang, Li Hua, Zhang Shu-Lin, Wang Yong-Liang, Kong Xiang-Yan, Zhang Chao-Xiang, Zhang Yong-Sheng, Xu Xiao-Feng, Yang Kang, Xie Xiao-Ming

Chin. Phys. B . 2015, 24(7): 078501. **doi:** 10.1088/1674-1056/24/7/078501

Micro-Gal level gravity measurements with cold atom interferometry

Zhou Min-Kang, Duan Xiao-Chun, Chen Le-Le, Luo Qin, Xu Yao-Yao, Hu Zhong-Kun

Chin. Phys. B . 2015, 24(5): 050401. **doi:** 10.1088/1674-1056/24/5/050401

Concept study of measuring gravitational constant using superconducting gravity gradiometer

Xing Bian(边星)[1,2,†], Ho Jung Paik[2], and Martin Vol Moody[3]

[1] *University of Chinese Academy of Sciences, Beijing* 100049, *China*
[2] *Technical Institute of Physics and Chemistry, Chinese Academy of Sciences, Beijing* 100190, *China*
[3] *Department of Physics, University of Maryland, College Park, Maryland* 20742, *USA*

(Received 20 April 2018; revised manuscript received 26 April 2018; published online 10 July 2018)

Newton's gravitational constant G is the least known fundamental constant of nature. Since Cavendish made the first measurement of G with a torsion balance over two hundred years ago, the best results of G have been obtained by using torsion balances. However, the uncorrected anelasticity of torsion fibers makes the results questionable. We present a new method of G measurement by using a superconducting gravity gradiometer constructed with levitated test masses, which is free from the irregularities of mechanical suspension. The superconducting gravity gradiometer is rotated to generate a centrifugal acceleration that nulls the gravity field of the source mass, forming an artificial planetary system. This experiment has a potential accuracy of G better than 10 ppm.

Keywords: gravitational constant, superconducting gravity gradiometer, artificial planetary system

PACS: 04.80.–y, 84.71.Ba, 85.25.Dq **DOI:** 10.1088/1674-1056/27/8/080401

1. Laboratory planetary system

Since Cavendish made his first measurement of Newton's gravitational constant G by using a torsion balance, over 300 new experiments have been carried out in the past 200 years to improve the accuracy. New technologies, such as microwave cavity, cold atom interferometry, and laser interferometry, have been used in the new experiments;[1–3] however, the torsion balance is still preferred. By measuring the period of a torsion balance in the gravity field produced by artificial gravity sources (time-of-swing method), the University of Washington gave the best result of G, of which the uncertainty is 14 ppm. This makes G the least known fundamental constant of nature.[4] Worse still, a number of results claiming uncertainty levels of 14 ppm–30 ppm disagree with each other by up to 10 standard deviations.[5] Kuroda pointed out that the anelasticity of torsion fibers produces a systematic error in the torsion balance experiments, which may be the reason for disagreements among the G values.[6] Experiments based on new principles other than the torsion balance are highly desirable in the determination of G.

A superconducting gravity gradiometer (SGG) is another powerful instrument for detecting weak gravity signals. The SGG developed at the University of Maryland (UM) did not reach a differential acceleration sensitivity of 4×10^{-12} m·s^{-2}·Hz$^{-1/2}$ until the early 1990's.[7] A new SGG with magnetically levitated test masses (TMs) under development at UM will improve the sensitivity by another two orders of magnitude and will be free from irregularities of the mechanical suspension since no mechanical springs are used.[8] Paik suggested a new way of measuring G based on a laboratory planetary system constructed with levitated superconducting TMs.[9] In this paper, we briefly describe a practical design of such an experiment and compute the expected resolution of the experiment. More details will be published elsewhere.

In a planetary system shown in Fig. 1(a), the gravity field of the central mass M is balanced by the centrifugal acceleration of the satellites.

$$GM/r^2 = r\omega^2, \tag{1}$$

where r and ω are the orbit radius and the angular velocity of the planet. From the orbital motions of the moon and the LAGEOS satellites, GM of the earth that has been determined to better than one part in 10^9.[10–12] Figure 1(b) shows the top view of a laboratory planetary system. The experiment is cooled to 4.2 K in a liquid helium dewar. The tungsten (W) sphere is the gravity source with mass M. Two magnetically levitated superconducting TMs are located at equal distance r from the source mass (SM). As M is moved up and down, perpendicular to the TM plane, we rotate the turntable with angular velocity ω to balance the change in the gravity field with centrifugal acceleration and keep the detector output constant. The value of G can now be determined only by measuring M, r, and ω. Measurement of the absolute gravity field is not needed; therefore, the calibration of the scale factor is unnecessary. This enables precise determination of G by using a superconducting gravity gradiometer.

†Corresponding author. E-mail: ciahpu@gmail.com

© 2018 Chinese Physical Society and IOP Publishing Ltd

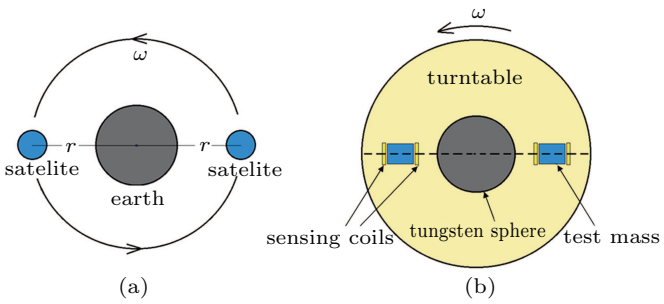


Fig. 1. (color online) (a) Two satellites orbiting the earth. (b) Two levitated test masses orbiting a tungsten sphere.

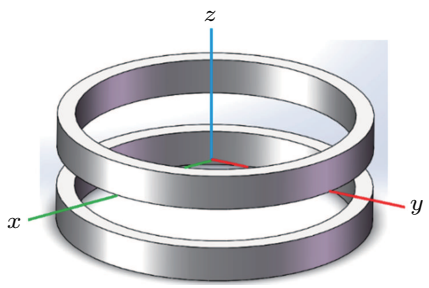


Fig. 2. (color online) Double-ring source

2. Experimental apparatus

2.1. Source mass

In the design of Fig. 1(b) and most of other G experiments, the positioning requirement of the TMs with respect to the SM is very severe. To reduce the positioning requirement, we design a double-ring tungsten SM as shown in Fig. 2, which is located outside the dewar. The outer diameter, inner diameter, thickness, and mass of each SM ring are chosen to be $D_{\rm RO} = 530$ mm, $D_{\rm RI} = 470$ mm, $h_{\rm R} = 60$ mm, and $M_{\rm R} = 54$ kg, respectively, the surface-to-surface separation of the two rings is $d = 90$ mm.

Figures 3(a) and 3(b) show the plots of the change of gravity field as a function of x and y, and as a function of x and z, respectively, in response to the SM displacement between levels $z_{\rm L}$ ($z = 0$) and $z_{\rm H}$ ($z = 4$ m). The middle parts of the plots are very flat, implying that the gravity gradients there are nearly constant. If we locate two TMs separated by baseline L in this area, $(g_{x2} - g_{x1})/L$ will be nearly insensitive to the TM positions along all x, y, and z directions, where g_{x1} and g_{x2} are the gravity field felt by TM 1 and TM 2, respectively. To make $\Delta g_x \equiv g_{x2} - g_{x1}$ least sensitive to their positions, the TMs are located at $P_1(-97.8$ mm, 0, 0) and $P_2(97.8$ mm, 0, 0), where the spatial derivative of the gravity gradient vanishes, as shown in Figs. 3(c) and 3(d). There we find $\Delta g_x = 3.12 \times 10^{-8}$ m·s^{-2}.

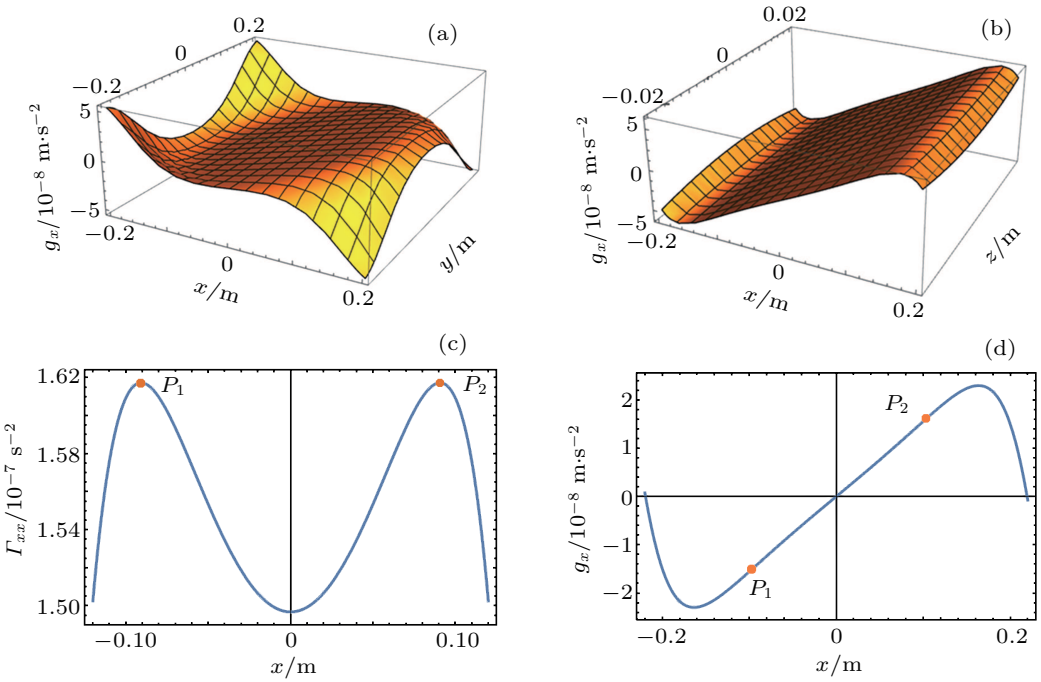


Fig. 3. (color online) (a) Gravity field versus x and y. (b) Gravity field versus x and z. (c) Gravity gradient at TM positions P_1 and P_2. (d) Gravity field at TM positions P_1 and P_2.

With the TM positions optimized, the relative positioning requirements of the source and the TMs corresponding to a G error of 3 ppm become $\leq \pm 6$ mm along the x axis, and $\leq \pm 1$ mm along the y and z axes, the relative orientation requirement becomes $\leq \pm 1.5$ mrad about the x and y axes. Comparing with the central SM design of Fig. 1(b), the positioning requirements are relaxed by four orders of magnitudes. The SM and TMs can now be aligned well within the required accuracy.

Figure 4 shows a cross-sectional view of the basic experimental apparatus. The SM position switches between height $z_{\rm L}$ and $z_{\rm H}$, and the resulting change in the differential gravity

between the two TMs is balanced by the centrifugal acceleration generated by rotating the detector about the z axis with the turntable. The value of G can be then determined from angular velocity ω, separation between the two TMs L, and the integrations of mass distributions of the SM and TMs over their volumes V_S and V_T:

$$\begin{aligned} &\Delta g_x(z_H) - \Delta g_x(z_L) \\ &= [g_{x2}(z_H) - g_{x1}(z_H)] - [g_{x2}(z_L) - g_{x1}(z_L)] \\ &= \omega^2 L, \end{aligned} \tag{2}$$

where

$$g_{xi}(z_j) = \frac{G}{V_{Ti}} \iiint \left[\iiint \rho_S \frac{\boldsymbol{r}_S - \boldsymbol{r}_T}{|\boldsymbol{r}_S - \boldsymbol{r}_T|^3} \mathrm{d}V_S(z_j) \right] \mathrm{d}V_{Ti} \quad (i = 1,2;\ j = H, L) \tag{3}$$

is the gravitational acceleration of the TM at P_i when the SM is at height z_j, ρ_S is the density of the SM, and $\boldsymbol{r}_S$ and $\boldsymbol{r}_T$ are the position vectors of the volume elements of the SM and TMs, respectively.

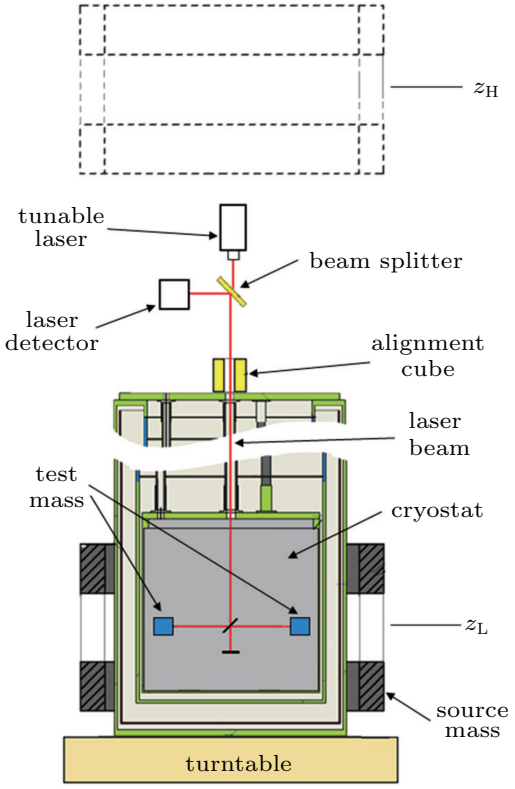


Fig. 4. (color online) Cross-sectional view of experiment apparatus.

2.2. Detector

The detector consists of two superconducting TMs levitated by currents induced along the levitation tube.[8] Figure 5(a) shows a perspective view of each TM. Figure 5(b) shows the TMs mounted on the Nb made detector platform, which houses superconducting circuits and optical components. The beam splitter and the mirror are for multicolor laser interferometry used to measure the absolute baseline between the TMs, which will be explained in Subsection 3.1. Each TM block is mounted on a cantilever spring. By adjusting the magnetic fields produced by the alignment coils behind the TM blocks, the sensitive axes are aligned to $< 10^{-5}$ rad. The detector is located inside a liquid helium dewar which is placed on a turntable.

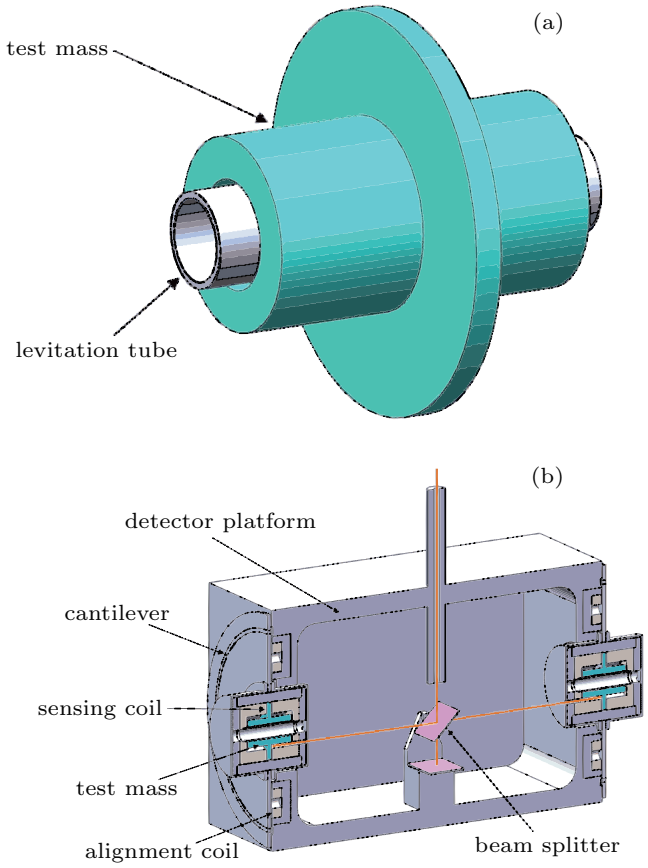


Fig. 5. (color online) (a) Test mass. (b) Test masses and optical components mounted on the detector platform.

To measure Δg_x, the two TMs are coupled with the superconducting circuit as shown in Fig. 6. Sensing currents I_1 and I_2 are stored in the coil loops for TM 1 and TM 2, respectively. The ratio I_2/I_1 is adjusted to make the output currents from the two loops in response to a common-mode (CM) acceleration cancel in the middle path. Only a differential-mode (DM) acceleration causes a current to flow in that path. A superconducting quantum interference device (SQUID) is coupled to this path to measure gravity gradient Γ_{xx}. This way the CM acceleration is rejected to 10^{-5}, limited by the misalignment of the sensitive axes of the two TMs. In addition, temperature sensing coil L_T is included to compensate for the error caused by the temperature fluctuation of the detector. By adjusting the persistent current I_T, the temperature sensitivity of the SGG is compensated to 10^{-3}. The details of the principle and design of the SGGs have been published in Refs. [7] and [8].

The intrinsic gradient noise power spectral density (PSD) of the SGG is[8]

$$S_\Gamma(f) = \frac{8}{mL^2}\left[k_B T\frac{\omega_0}{Q} + \frac{(\omega^2-\omega_0^2)^2}{2\beta\eta\omega_0^2}E_A(f)\right], \quad (4)$$

where m is the mass of each TM, L is the baseline, k_B is the Boltzmann constant, T is the temperature, ω_0 and Q are the DM (angular) resonance frequency and quality factor respectively, $\beta\eta$ is the test-masses-to-SQUID energy coupling constant, $E_A(f)$ is the SQUID input energy resolution, and $f = \omega/2\pi$ is the signal frequency. With $Q = 10^6$, $m = 27$ g, $L = 195.6$ mm, $f_0 = 0.3$ Hz, $T = 4.2$ K, $\beta\eta = 0.25$, and $E_A(f) = 1\times10^{-30}(1+0.5\text{ Hz/f})$ J/Hz, we obtain $S_\Gamma^{1/2}(f) = 4.8\times10^{-12}\text{ s}^{-2}\cdot\text{Hz}^{-1/2}$ at $f = 0.046$ mHz.

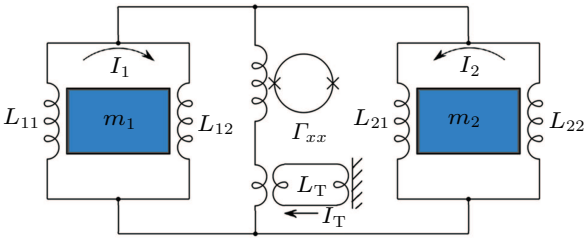


Fig. 6. (color online) Schematic circuit diagram of the SGG.

3. Experimental procedure

3.1. Measurements of absolute distances

To determine G, we need to measure the absolute lengths of the SM and TMs, as well as the length of the baseline between the two TMs.

The gravity signal is very sensitive to the average diameter and separation between the SM rings. With a coordinate measurement machine (CMM),[13] the SM dimensions D_{RO}, D_{RI}, H_R, and d can be determined to 0.83 μm, 0.77 μm, 0.36 μm, and 0.39 μm, respectively. These SM metrology errors make a dominant contribution to the G error: $\Delta G/G = 3.6$ ppm. For the TMs, since their dimensions are small and the gravity gradient is uniform (see Fig. 3), the TM metrology errors make a negligible contribution: $\Delta G/G < 0.01$ ppm.

The detector baseline is given by

$$L = L_{ss} + d_{V1}/2 + d_{V2}/2, \quad (5)$$

where L_{ss} is the surface-to-surface distance between the two central vanes of the TMs, d_{V1} and d_{V2} are the thickness values of the two central vanes (see Fig. 7). We use the synthetic wavelength laser interferometry[14] to determine L_{ss}. By repeating the measurement four times with three different wavelengths generated by a tunable laser, and comparing the fringe patterns, we are able to determine L_{ss} to 0.34 μm. Combining the uncertainties of L_{ss}, d_{V1} and d_{V2}, we find the error in the baseline measurement: $\delta L = 0.4$ μm. This corresponds to $\Delta G/G = 2$ ppm. The baseline error caused by the deviation of the central vane positions from the midplane can be averaged out by repeating the experiment with both TMs flipped about the z axis and averaging the results.

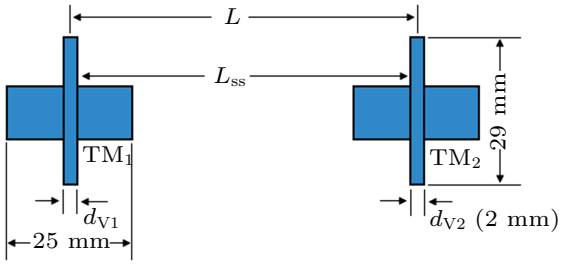


Fig. 7. (color online) Test mass dimensions and the baseline.

3.2. Determination of density inhomogeneities

Density inhomogeneities of the SM and TMs result in errors in the computation of the gravity signal. To estimate these errors, the SM and TMs are divided into 1 mm×1 mm×1 mm cubes, each with a randomly generated density with standard deviation $\sigma(\Delta\rho/\rho) = 1\times10^{-3}$, which is a very conservative estimate.[15] We find that the density inhomogeneity of the SM causes an uncertainty of 7.2 nm in the average SM diameter and an uncertainty of 14 nm in the separation between the two SM rings, corresponding to $\Delta G/G$ of 0.027 ppm and 0.098 ppm, respectively.

For the TMs, the density inhomogeneity causes uncertainties in mass center position of $\delta x_T = 82$ nm along the x axis and $\delta y_T = \delta z_T = 91$ nm along the y and z axes. δx_T can be averaged out by repeating the experiment with the TMs flipped about the z axis and averaging the results. Further, $\Gamma_{yx} = \Gamma_{zx} = 0$ in the geometry center of the TMs and $< 2\times10^{-9}$ s^{-2} over the entire space occupied by the TMs (see Section 2). The residual $\Delta G/G$ caused by the TM density inhomogeneity is < 0.01 ppm.

3.3. Measurement of angular velocity

Due to the weak gravity signal, the turntable rotates so slowly that signal frequency f_s is deep inside the $1/f$ noise region of the SQUID. At low frequencies, atmospheric pressure fluctuation also increases, causing higher temperature fluctuation of the helium bath. The temperature drift is the main source of output drift of the SGG. So it is very desirable to perform the experiment at a higher frequency. We employ a precision optical cube to increase f_s by a factor of 4, and use bias angular velocity Ω_b to increase f_s further.

As shown in Fig. 8, the laser beam from the autocollimator is reflected by the alignment cube and the reflected beam is aligned with the incident beam every $\pi/2$ of rotation. The time

intervals are recorded to calculate the average angular velocities. Commercial precision alignment cubes are accurate to $5\times10^{-6}-10^{-5}$ rad. This error can be reduced to $<10^{-6}$ rad by repeating the experiment over each quadrant of the cube and averaging the results, because the deviation of the sum of the four interior angles from 2π is a second-order effect.

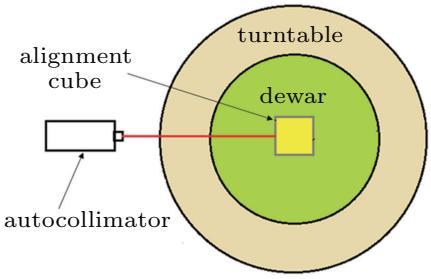


Fig. 8. (color online) Turntable with an optical cube.

With the SM at $z_{\rm L}$, we control the angular velocity of the turntable Ω to keep the detector output constant, and measure t_1, the time that is taken for the turntable to cover the first quadrant (0°–90°). Then, we move the SM slowly from $z_{\rm L}$ to $z_{\rm H}$ in the second quadrant (90°–180°) while increasing Ω gradually and measure time interval t_2. We again control Ω to keep the detector output constant in the third quadrant (180°–270°) and measure t_3. Since Ω cannot be controlled accurately during the second quadrant, we exclude this part from the data analysis. The change of centrifugal acceleration in response to the displacement of the SM is

$$\Delta g_x(z_{\rm H})-\Delta g_x(z_{\rm L})=L[(\Omega_{\rm b}+\Delta\Omega)^2-\Omega_{\rm b}^2], \tag{6}$$

where $\Omega_{\rm b}=\pi/2t_1$ and $(\Delta\Omega+\Omega_{\rm b})=\pi/2t_3$ are the average angular velocity in the first and third quadrant, respectively. With $\Omega_{\rm b}=0.2$ mrad/s, we find $(\Delta\Omega+\Omega_{\rm b})=0.45$ mrad/s and $f_{\rm s}=1/(t_1+t_3+2t_2)=0.046$ mHz. This method gives an additional advantage of canceling the gravity gradient background of the laboratory precisely because the gravity gradient in the first and the third quadrant is the same due to its rotational symmetry.

To reduce the angle error of the alignment cube, we need to repeat the measurement four times to cover all four quadrants, and to average out the density inhomogeneity and metrology error of the TMs along the x axis, we flip the TMs about the z axis and repeat the experiment. So we will repeat the measurement run eight times in total.

4. Experimental errors

With the SGG output fed back to the turntable, gravity gradient noise $\Gamma_N(t)$ will cause noise in the instantaneous angular velocity, resulting in an error in the average angular velocity. We find that the error in the differential gravity measurement caused by $\Gamma_N(t)$ becomes

$$\delta g=L[S_\Gamma(f_{\rm s})\Delta f/2]^{1/2}, \tag{7}$$

where $\Delta f=f_{\rm s}/16$ is the bandwidth for eight runs. Substituting

$$S_\Gamma^{1/2}(f_{\rm s})=4.8\times10^{-12}\ {\rm s}^{-2}\cdot{\rm Hz}^{-1/2},$$

the detector intrinsic noise at 0.046 mHz, into Eq. (8), we obtain 5.7×10^{-15} m·s^{-2}. This corresponds to $\Delta G/G$ of 0.18 ppm.

Similarly, the seismic noise, $\sim3\times10^{-7}$ m·s$^{-2}\cdot$Hz$^{-1/2}$ at 0.046 mHz,[16] rejected by CM rejection ratio 10^5 and summed over three axes, results in a differential acceleration error of 6.2×10^{-15} m·s^{-2}, corresponding to $\Delta G/G$ of 0.2 ppm.

The atmospheric pressure fluctuation causes a helium boiling point fluctuation of 18.8 mK·Hz$^{-1/2}$ at 0.046 mHz.[17] The temperature fluctuation causes an error in the SGG due to the temperature sensitivity of the superconducting penetration depth.[7] With the temperature compensation feature in the sensing circuit (Fig. 6), we will be able to reduce the temperature-to-displacement sensitivity by three orders of magnitude to 1.5×10^{-11} m·K^{-1}, which causes a differential acceleration noise of 1.1×10^{-12} m·s$^{-2}\cdot$Hz$^{-1/2}$. This corresponds to $\Delta G/G=0.06$ ppm. In addition, the temperature fluctuations of the laboratory causes the SM dimension to vary. Assuming that the temperature of the laboratory is controlled to 1 °C and that 5% of the temperature variation occurs at our signal frequency band, we find $\Delta G/G=0.83$ ppm.

As explained in Section 3, we will difference the average angular velocity signals measured over the first and the third quadrant to determine the gravity signal. In addition to the SGG noise affecting the angular velocity of the turntable, which is given by Eq. (8), the angular error in the optical cube and the error in the autocollimator reading contribute measurement errors of angular velocity. We find that the gravity gradient error caused by the average angular velocity measurement errors is

$$\Gamma_{\rm av}=\Gamma_{\rm s}-\Gamma_m=\sqrt{16\theta_{n0}^2\left(\Gamma_{\rm s}+2\Omega_{\rm b}^2\right)^2/\pi^2+2\theta_n^2\left(\Gamma_{\rm s}^2+2\Gamma_{\rm s}\Omega_{\rm b}^2+2\Omega_{\rm b}^4\right)/\pi^2}, \tag{8}$$

where $\theta_{n0}=10^{-6}$ rad is the residual angle error of the optical cube after averaging over the four quadrants, and $\theta_n=2.4\times10^{-7}$ rad is the repeatability of the autocollimator.[18] We thus obtain $\Gamma_{\rm av}=3.1\times10^{-13}$ s^{-2}. This results in $\Delta G/G=1.9$ ppm.

5. Expected resolution

In Table 1, we list all the errors. Assuming that the errors are uncorrelated, we obtain a total error of $\Delta G/G = 4.9$ ppm by the root sum square of the errors. The SM metrology error dominates the error budget of the proposed experiment. The detector noise makes a very small contribution.

Table 1. Instrument errors and noises of the proposed G experiment.

Category	Error source	Uncertainty	$\Delta G/G$
Dimensions and angles	Source mass dimensions	0.36 μm–0.83 μm	3.6 ppm
	Test mass dimensions	0.56 μm	< 0.01 ppm
	Detector baseline L	0.40 μm	2.0 ppm
	Optical cube	10^{-6} rad	1.9 ppm
	Angle measurement	2.4×10^{-7} rad	0.14 ppm
Mass	Source mass	0.1 g	1.0 ppm
Density inhomogeneity	Source mass	1×10^{-3}	0.1 ppm
	Test mass	1×10^{-3}	< 0.01 ppm
Source-detector alignment	x axis	0.55 mm	< 0.01 ppm
	y axis	0.55 mm	0.8 ppm
	z axis	0.51 mm	0.95 ppm
	Parallelism	0.50 mrad	0.66 ppm
Noise	Detector intrinsic	4.8×10^{-12} m·s^{-2}·Hz$^{-1/2}$	0.18 ppm
	Seismic	3×10^{-7} m·s^{-2}·Hz$^{-1/2}$	0.2 ppm
	Detector temperature	20 mK·Hz$^{-1/2}$	0.06 ppm
	Source temperature	0.05 K	0.83 ppm
Total error			4.9 ppm

6. Conclusions

In this paper, we present a design of a new experiment, which has the potential of measuring gravitational constant G to < 10 ppm. The gravity signal is generated by a double-ring shaped SM, which relaxes the relative positioning requirement between the SM and the detector to a manageable level. The gravity signal is detected by an SGG constructed with two levitated TMs, which has very low noise, high CM rejection capability, with no anelasticity or other irregularities associated with mechanical springs. The gravity signal is balanced by a centrifugal acceleration generated by rotating the detector, thus the apparatus forms an artificial planetary system. The SGG acts as a null detector, so its scale factor calibration is unnecessary. All the detector technologies used in this experiment have already been developed with the SGG development at UM.

Acknowledgment

We thank Riley Newman and Jun Luo for the useful discussion about gravity measurement, and also Ziren Luo and Suwen Wang for the optical design and angular velocity measurement. We benefited from the collaboration with Cornelius Griggs and Ron Norton. Xing Bian especially benefited from his one-year visit to the UM Gravitation Laboratory, during which period the design of the G experiment reported in this paper was studied.

References

[1] Kleinevoss U, Meyer H, Schumacher A and Hartmann S 1999 *Meas. Sci. Technol.* **10** 492
[2] Rosi G, Sorrentino F, Cacciapuoti L, Prevedelli M and Tino G M 2014 *Nature* **510** 518
[3] Schwarz J P, Robertson D S, Niebauer T M and Faller J E 1998 **282** 5397
[4] Gundlach J H and Merkowitz S M 2000 *Phys. Rev. Lett.* **85** 2869
[5] Reich E S 2010 *Nature* **466** 1030
[6] Kuroda K 1995 *Phys. Rev. Lett.* **75** 2796
[7] Moody M V, Paik H J and Canavan E R 2002 *Rev. Sci. Instrum.* **73** 3957
[8] Griggs C E, Moody M V, Norton R S, Paik H J and Venkateswara K 2017 *Phys. Rev. Appl.* **8** 064024
[9] Paik H J 2000 talk presented at an invited session "Modern G measurements" at the *American Physical Society Meeting*, 2000, Long Beach, USA
[10] Smith D E, Christodoulidis D C, Kolenkiewicz R, Dunn P J, Klosko S M, Torrence M H, Fricke S and Blackwell S 1985 *J. Geophys. Res.: Solid Earth* **90** 9221
[11] Lerch F J, Laubscher R E, Klosko S M, Smith D E, Kolenkiewicz R, Putney B H, Marsh J G and Brownd J E 1978 *Geophys. Res. Lett.* **5** 1031
[12] Ries J C, Eanes R J, Huang C, Schutz B E, Shum C K, Tapley B D, Watkins M M and Yuan D N 1989 *Geophys. Res. Lett.* **16** 271
[13] Hexagon Manufacturing Intelligence http://www.hexagonmi.com/products/coordinate-measuring-machines/bridge-cmms/leitz-infinity [2018]
[14] Alzahrani K, Burton D, Lilley F, Gdeisat M, Bezombes F and Qudeisat M 2012 *Opt. Express* **20** 5658
[15] Liu L X, Shao C G, Tu L C and Luo J 2009 *Chin. Phys. Lett.* **26** 010403
[16] Zürn W and Wielandt E 2007 *Geophys. J. Int.* **168** 647
[17] Herron T J, Tolstoy I and Kraft D W 1969 *J. Geophys. Res.* **74** 1321
[18] AcroBeam http://www.acrobeam.com/Html/Product/product1/230.html [2018]